Optical Properties of Aligned Rod-Shaped Gold Particles Dispersed in Poly(vinyl alcohol) Films

Bianca M. I. van der Zande,*,†,‡ Laurent Pagès,‡ Rifat A. M. Hikmet,‡ and Alfons van Blaaderen*,†,§

Van 't Hoff Laboratory for Physical and Colloid Chemistry, Debye Institute, Utrecht University, Padualaan 8, 3584 CH Utrecht, The Netherlands, Philips Research Laboratories, Prof. Holstlaan 4, 5656 AA Eindhoven, The Netherlands, and FOM-Institute for Atomic and Molecular Physics, Kruislaan 407, 1098 SJ Amsterdam, The Netherlands

The polarization spectra of template-synthesized colloidal gold rods with aspect ratios ranging from $L/d =$ 1.8 to 49 (and a diameter $d = 15$ nm) embedded in poly(vinyl alcohol) (PVA) films are studied as a function of the film elongation. Orientation of the colloidal gold rods is obtained by stretching the PVA films. The polarization absorbance spectra of aligned systems show only one resonance band instead of two absorbance bands as found for randomly distributed gold rods. The visible and near-infrared spectra reveal that the rods are completely oriented when the film is stretched 4−6 times its original length. No significant effect of the aspect ratio is observed on the film elongation required for complete alignment. The alignment of gold rods by the stretched-film method is visualized by reflection confocal scanning laser microscopy (CSLM). The CSLM micrographs also demonstrate the distribution of single gold rods in the film.

Introduction

The optical properties of metal colloids have attracted a considerable interest because of the bright colors of the dispersions.[1−3] The optical properties of rod-shaped particles are of interest,[4−12] because the absorbance spectrum of randomly distributed rod-shaped particles displays a longitudinal and a transverse resonance[4−12] instead of one absorbance maximum for colloidal spheres. The two plasmon resonances originate from the two components of the electric field of the incident light perpendicular and parallel to the main axis of the particle.[13−15]

The magnitude of both the longitudinal and transverse resonance is sensitive to the orientational order of the rod-shaped particles. When the incident light is polarized parallel to the main axes of the particles, which are fully aligned, the spectrum displays only the longitudinal resonance. In the case of light polarized perpendicular to the main axes of the rod-shaped particles which are fully aligned, the spectrum displays only the transverse resonance. The aim of this study is to investigate the optical properties of anisotropic gold particles embedded in poly(vinyl alcohol) films as a function of the net orientation of the rods at a fixed polarization angle. Alignment of the colloidal gold rods in a preferred direction was obtained by use of the stretched-film method.[16−18] The results obtained for the alignment of gold rods in electric fields are reported in ref 19. In ref 20 the optical properties of fully aligned gold rods have been studied extensively as a function of the polarization angle. A strong dependence of the absorbance on the polarization angle was found.

The orientation and distribution of the rods in the stretched and unstretched films are visualized with reflection scanning

confocal light microscopy (CSLM). Confocal microscopy has several advantages over ordinary light microscopy due to the extremely limited field of view.[21,22] Only a diffraction limited point is focused inside the sample and the reflection is subsequently imaged through the same lens on a point detector.[21] This mode of imaging causes a strong depth discrimination. By scanning the beam over a 2D plane, an optical section with a thickness of typically 500 nm and an in-plane resolution of 250 nm is created. This resolution is sufficient to observe the orientation of the gold rods if the interparticle distance is larger than the in-plane resolution.

Experimental Section

Aqueous Dispersions of Rod-Shaped Gold Particles. The gold dispersions of rod-shaped particles with aspect ratios in the range $1.8 < L/d < 49$ were synthesized as described in refs 4 and 23. This reproducible method enables the preparation of rods with an adjustable aspect ratio. Poly(vinyl pyrrolidone) (K30−PVP, $M_w = 40\,000$, Fluka) was used as a stabilizer. The thickness of the polymer layer is about $10−15$ nm.[24] The colloidal stability of the dispersions is investigated with dynamic light scattering and electrophoresis as described in ref 24. There, it is concluded that the dispersions exhibit colloidal stability. Spherical gold particles with $d = 17$ nm were prepared following the method of Frens.[25] The dispersion of these particles served as a reference. Table 1 summarizes the average particle dimensions of the dispersions determined by transmission electron microscopy (TEM) analysis. The total gold concentration of the aqueous dispersions of gold particles was measured by inductively coupled plasma optical emission spectroscopy.[23,24] The gold concentration was about $10^{-5}−10^{-4}$ g·mL^{-1}.

Preparation of PVA Films Containing Gold Particles. The PVA films in which the gold particles are embedded were cast from an ethylene glycol (Merck) solution containing 5% PVA ($M_w = 85\,000−146\,000$, 98−99% hydrolyzed, Aldrich) and

† Utrecht University.
‡ Philips Research Laboratories.
§ FOM-Institute for Atomic and Molecular Physics.

**TABLE 1: Characteristics of the Template-Synthesized Gold Rod Dispersions**[a]

no.	L (nm)	σ_L (nm)	d (nm)	σ_d (nm)	L/d
1			17	4	
2	40	8.5	22	4.3	1.8
3	82	9.4	19	3.4	4.4
4	259	54	15	2.4	17.2
5	380	50	20	4	19
6	729	20	15	3	49

[a] The particle dimensions are determined by TEM analysis. L = the number-averaged particle length. d = the number-averaged diameter. σ_x = the standard deviation of x.

gold particles. The gold particles were transferred from water to ethylene glycol by adding 3 mL of ethylene glycol to the aqueous dispersion. The water was evaporated in an oven at 105 °C. We checked whether the water was totally evaporated by weighing. To ensure colloidal stability in ethylene glycol an additional amount of the stabilizer PVP has to be added to the aqueous dispersion. The additional amount of stabilizer was kept constant for all dispersions, 0.35 mL of 2 g·L^{-1} of PVP solution. In this way the final PVP concentration in the PVA films was approximately the same for each film. After the weight of the dispersion had become constant (about 2.8 g), 0.1 g of PVA was added to the ethylene glycol dispersion and the mixture was heated to 195 °C. The PVA was completely dissolved after 30−60 min of gentle stirring, resulting in a solution with a high viscosity. During this stirring stage, 1 mL of ethylene glycol evaporated. The final concentration of PVA was about 5 (w/w)%. When the PVA was dissolved, the solution was poured on a glass plate, resulting in a mechanically weak film that crystallized immediately due to the decrease in temperature.[27] After 45 min of drying in the open air, the film was placed into methanol for at least 2 h. Methanol replaces the ethylene glycol and facilitates the hardening of the film. The film was dried at room temperature for 6 days. During the drying process the film was clamped to prevent retraction. The thickness of the PVA films was in the range of 40−90 μm, as determined by CSLM. The gold concentration per PVA film area is estimated to be 25−30 μg·cm^{-2}. The volume percentage has to be low to prevent multiparticle interactions and changes in the refractive index of the medium.[28−30]

Orientation of the colloidal gold rods in a particular direction was obtained using the stretched-film method.[16,17] The stretching of the film was performed by putting a piece of the film on a hot plate at 120 °C to soften the film followed by mechanically stretching with two clamps until the desired elongation was reached. In the following we denote the extent of elongation as for instance 2 times stretched, which indicates that the film was twice its original length. The elongation number is in that case 2. The maximum elongation obtained was 10 times the films original length.

Measurements. *Absorbance.* The absorbance spectra of randomly oriented gold rods were recorded on a Perkin-Elmer UV/VIS/NIR Lambda 9 double-beam spectrophotometer using unpolarized light in the wavelength regime from 400 to 1350 nm. The absorbance spectra of oriented gold rods in stretched PVA films were measured with a single beam ultraviolet visible (UV/VIS) spectrophotometer (UNICAM series 8700) in the wavelength regime from 400 to 770 nm. A vis polarizer (230−770 nm, Oriel) was mounted in front of the sample. The stretched films were attached on a diaphragm with a hole diameter of 3 mm. All spectra were measured at two polarization angles $\Psi = 0°$ and $\Psi = 90°$. At $\Psi = 0°$ the incident wave vector of light was parallel to the stretch direction. Figure 1
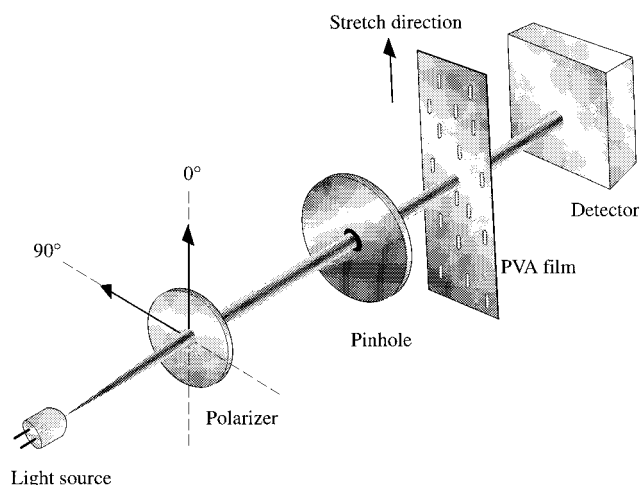
Figure 1. Optical set up. At a polarization angle $\Psi = 0°$ the electric field of the light is polarized parallel to the stretch direction, whereas at a polarization angle $\Psi = 90°$ the electric field of the light is polarized perpendicular to the stretch direction.

shows the optical set up schematically. The baseline was drawn in air with the polarizer rotated in the direction of the polarization of the subsequent measurement.

For the PVA films in which the $L/d = 4.4$, gold rods were dispersed, the behavior of the longitudinal resonance, which occurs in the wavelength regime $\lambda > 700$ nm, was monitored on a Perkin-Elmer UV/VIS/NIR Lambda 9 double-beam spectrophotometer by use of an IR polarizer (780−1250 nm, Melles Griot). No diaphragm was used in this particular case.

Confocal Scanning Laser Microscopy (CSLM). CSLM measurements were performed in the reflection mode with a Leica TCS NT confocal microscope equipped with a krypton/argon gas laser and an oil immersion lens (numerical aperture 1.4, lateral resolution of 0.2 μm, and axial resolution of 0.65 μm). Reflection measurements were made using a wavelength of 488 nm and a combination of a quarter wave plate and analyzer to reduce reflections in the optical train of the microscope. Furthermore, the refractive index of the film material is close to that of glass. This minimizes optical distortions and allows imaging of the rods throughout the entire thickness of the film. The film wetted with immersion oil was sandwiched between two glass plates. A 3D image could be constructed by digital image analysis with the stored data of approximately 70 parallel cross sections with an area of 50 μm × 50 μm over a depth of 30−40 μm.

Results and Discussion

Optical Properties of Randomly Oriented Gold Particles. Figure 2 shows the absorbance spectra of randomly oriented gold rods in water and in PVA films. Two maxima were found. The maximum around $\lambda = 520$ nm is the transverse plasmon resonance,[4,5,13,28] and the more pronounced second absorbance maximum is the longitudinal plasmon resonance.[4−12] The longitudinal resonance of the dispersion with rods of $L/d = 17.2$ occurs at $\lambda > 1300$ nm, which is outside the experimental range. Consequently, we could not monitor this resonance. The spectra of the PVA films agree with those of the aqueous systems with the exception of a peak shift to longer wavelengths due to the change in refractive index of the medium. Peak broadening does not occur, indicating that the colloidal gold rods are well-dispersed in PVA.

To verify whether the absorbance behavior of the PVA films indeed corresponds with well-dispersed colloidal gold rods, we

Optical Properties of Aligned Au Particles

J. Phys. Chem. B, Vol. 103, No. 28, 1999 **5763**
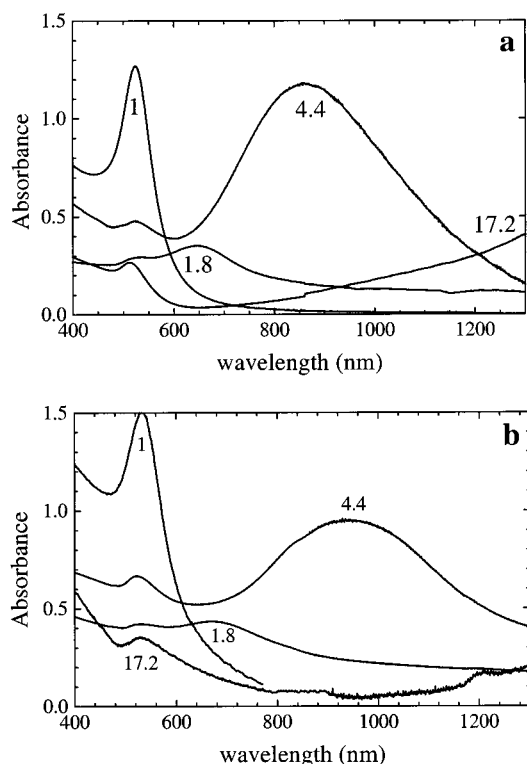
Figure 2. The absorbance behavior of randomly oriented gold rod dispersions. Figure 2a shows the absorbance spectra of the aqueous dispersions and Figure 2b the spectra of gold rods dispersed in PVA. The spectra of gold spheres indicated with (1) are given as well. The numbers on the spectral curves represent the aspect ratio.

have calculated the peak positions using the expressions of Gans,[13–15] which are summarized in Appendix I. The optical parameters for bulk gold are taken from ref 31. The refractive index of the medium was assumed to be constant and equals 1.519 for PVA[11] and 1.333 for H_2O. In ref 5 it is demonstrated that the Gans theory can be used to predict the positions of the absorbance maxima, although the particles have dimensions on the order of the wavelength of light. The optical behavior of the stable aqueous dispersions[24] of gold rods complies with the theoretical predictions. The small deviations (indicated with Δ in Table 2) are attributed to the polydispersity in shape.[5] Table 2 summarizes the positions of the experimental absorbance maxima as well as those theoretically predicted (eq 1). The small deviations in the transverse and longitudinal peak positions for the PVA systems are similar to the deviations found for the aqueous systems. This supports that the colloidal gold rods are well-dispersed in the PVA films.

Optical Properties of Aligned Gold Rods Dispersed in PVA Films. Figure 3 shows the absorbance spectra of a PVA film. The absorbance is monotonically decreasing with increasing wavelength due to scattering contributions. The control of the film thickness is, however, not good enough to prevent scattering contributions that vary along the film and with elongation number. The consequence of the uncontrolled thickness of the PVA film is that we cannot draw conclusions from the absolute values of the absorbance. Therefore, only the peak heights at a particular orientation can be compared in the following.

The polarization spectra of the investigated dispersions: spheres with $d = 17$ nm, $L/d = 1.8$, $L/d = 4.4$, and $L/d = 17.2$ are given in Figures 4, 5, 6, and 7, respectively. The spectral curves are arbitrarily shifted along the y-axis for the sake of clarity. The elongation number increases from the upper to the

TABLE 2: Positions of the Experimental (λ_{exp}) and Calculated (λ_{cal}) Absorbance Maxima[a]

	transverse resonance			longitudinal resonance		
L/d	λ_{exp} (nm)	λ_{cal} (nm)	Δ (nm)	λ_{exp} (nm)	λ_{cal} (nm)	Δ (nm)
	H_2O ($n = 1.333$)					
1 (sphere)	523	521	2			
1.8	531	518	13	646	585	61
4.4	518	506	12	860	830	30
17.6	512	503	9	>1350	>2000	
19	520	503	17	>1350	>2000	
49	512	503	9	>1350	>2000	
	PVA ($n = 1.519$)					
1 (sphere)	531	533	−2			
1.8	531	525	6	670	610	60
4.4	521	515	6	945	920	25
17.6	526	510	16	>1350	>2000	
19	528	510	18	>1350	>2000	
49	520	510	10	>1350	>2000	

[a] The calculations are performed with eq a1 using the optical parameters of bulk gold from ref 31. The refractive index of the medium is assumed to be constant in the visible near infrared wavelength regime, 1.333 for water and 1.519 for PVA.[11] The difference between the peak positions measured and predicted is given by $\Delta = \lambda_{exp} - \lambda_{cal}$.
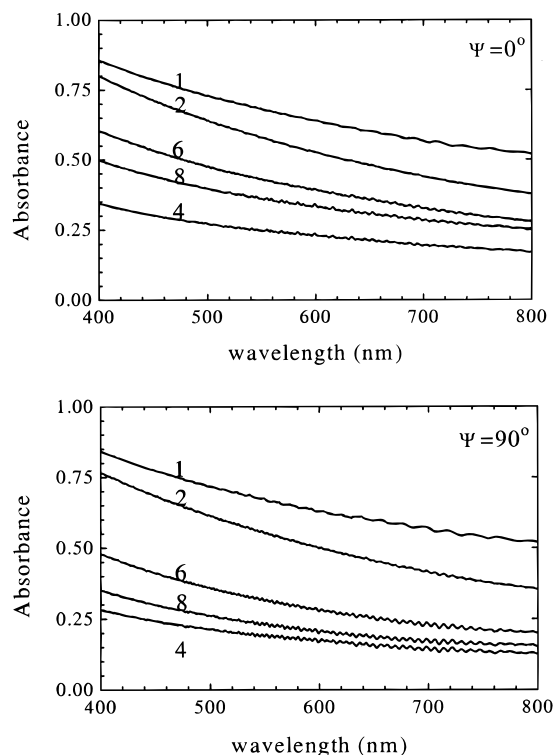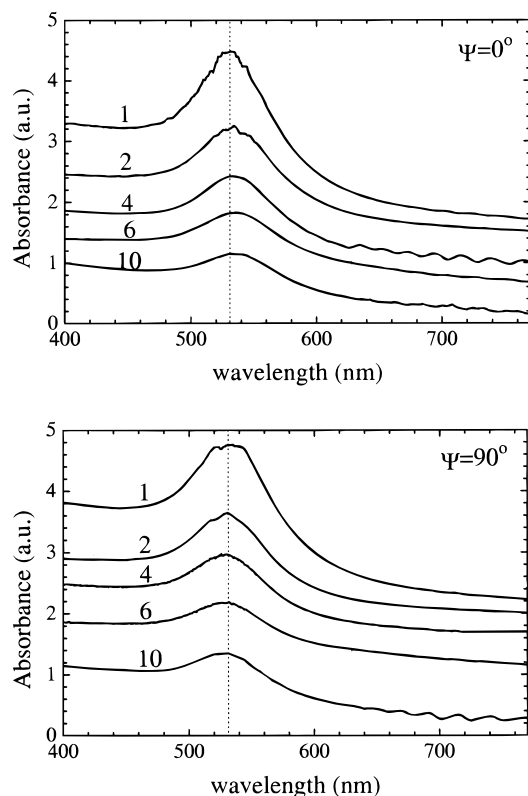

Figure 3. The absorbance spectra of a PVA film without gold particles for various elongation numbers indicated on the spectral curve. The polarization angle, Ψ, is given in the figure. Note that the absolute values depend on the position of the film with respect to the incident light.

lowest spectrum. The numbers on the spectral curves represent the elongation with respect to the original film.

The polarization spectra of the film containing colloidal gold spheres (Figure 4) show an absorbance maximum at both polarization angles. As expected, the optical behavior of colloidal spheres is independent of the direction of the incident wavevector of light because of the spherical symmetry. The decrease of the peak height is attributed to the decrease in film thickness by stretching. The exact peak position, however, depends on the elongation and polarization direction due to the birefringence of the PVA film.[27,32,33] In the parallel polarization

Figure 4. The polarization spectra of the gold spheres with $d = 17$ nm dispersed in PVA for various elongation numbers indicated on the spectral curves. The curves are arbitrarily shifted along the y-axis for the sake of clarity. The polarization angle, Ψ, is given in the figure.
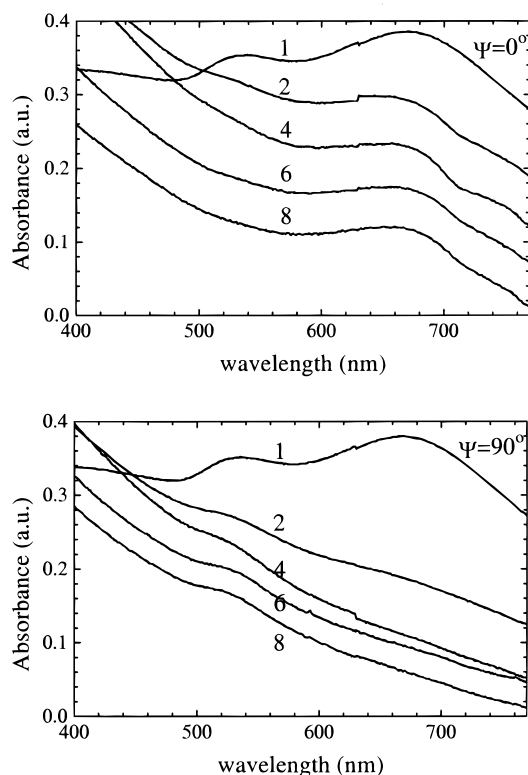
Figure 5. The polarization spectra of the $L/d = 1.8$ rods dispersed in PVA for various elongation numbers indicated on the spectral curves. The curves are arbitrarily shifted along the y-axis for the sake of clarity. The polarization angle, Ψ, is given in the figure.

($\Psi = 0°$), the absorbance maxima positions shift slightly to longer wavelengths with increasing elongation number, while

in the perpendicular polarization ($\Psi = 90°$), a slight shift to shorter wavelengths occurs. At an elongation of 6, the former shift equals 3 nm and the latter 2 nm. Using the PVA birefringence data of ref 28, we recalculated the refractive index of the stretched PVA films for both polarization directions. The difference between the calculated positions of the parallel and perpendicular polarized absorbance maxima and the refractive index corrected for birefringence is similar to the difference found in the present study and equals 5 nm. In addition, XRD analysis confirmed the increase in crystalline order by stretching.
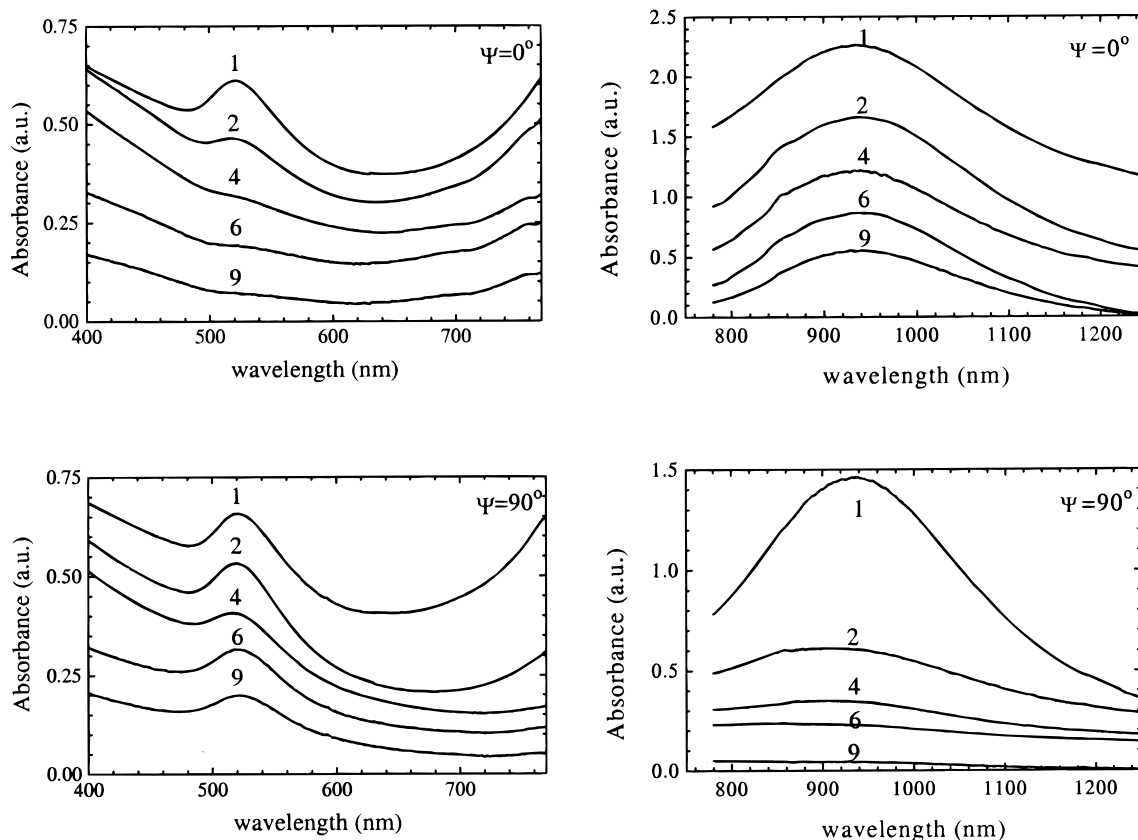
Figure 5 shows the polarization spectra of the films containing rod-shaped gold particles with $L/d = 1.8$. The spectra demonstrate that at parallel polarization ($\Psi = 0°$) the transverse absorbance maximum completely disappears when the film is stretched 4−6 times, whereas the longitudinal resonance is still present. Note that the longitudinal resonance is less pronounced, because of the decrease in film thickness analogous to the peak height of spheres. Using perpendicular polarized light ($\Psi = 90°$), only the transverse resonance appears at maximum elongation. Changes from blue to red were observed by switching the polarizer from the parallel to the perpendicular polarization direction, respectively.

Similar trends are seen for the gold rods with $L/d = 4.4$, shown in Figure 6. The spectrum is split up in two parts (400−800 and 750−1250 nm) because of the range of the polarizer. The spectrum recorded in the wavelength regime 400−800 nm shows the behavior of the transverse resonance as function of the elongation, and that recorded in the regime 750−1250 nm shows the longitudinal resonance. Figure 6 demonstrates that at a polarization angle $\Psi = 0°$ the absorbance of stretched films is caused by the longitudinal resonance. The transverse resonance still shows a weak shoulder at an elongation of 4, but it completely vanishes when the film is stretched 6 times. At $\Psi = 90°$ the longitudinal resonance vanishes, while the transverse resonance is unaffected. The spectral curves point to alignment of the particles.

Finally, Figure 7 shows the polarization spectra of rods with $L/d = 17.2$. The longitudinal resonance of the $L/d = 17.2$ rods cannot be monitored, because the absorbance maximum position falls outside the scope of the experimental wavelength regime. Nevertheless, the transverse resonance shows a similar behavior as found for the rod system $L/d = 4.4$. A weak shoulder of the transverse resonance is still present at an elongation of 4, but it disappears after the film was stretched 4−6 times. The same behavior is found for the PVA films in which rods with $L/d = 19$ and 49 are embedded.

Al-Rawashdeh et al.[20] studied the polarization spectra of *aligned* colloidal gold rods dispersed in polyethylene as function of the polarization angle. Our results show a strong analogy with the results of Al-Rawashdeh et al.[20] obtained for gold rods with $d = 16$ nm and $L/d = 2.2$ and 6.3. Al-Rawashdeh et al.[20] obtained only the longitudinal resonance at $\Psi = 0°$ and only the transverse resonance at $\Psi = 90°$ as we did when the films were stretched 4−6 times its original length. In the case of polarization angles between $0°$ and $90°$, both resonances contributed to the absorbance of light,[20] which is in accordance with the results we obtained for unstretched films and films with an elongation value of 2.

Visualization of the Particle Orientation. The orientation of particles with $L/d = 19$ and 49 could be visualized with CSLM. Figure 8 shows a sequence of CSLM micrographs of the film containing rods with $L/d = 49$ obtained using light with $\lambda = 488$ nm. The polarization spectra are given in Figure

Optical Properties of Aligned Au Particles

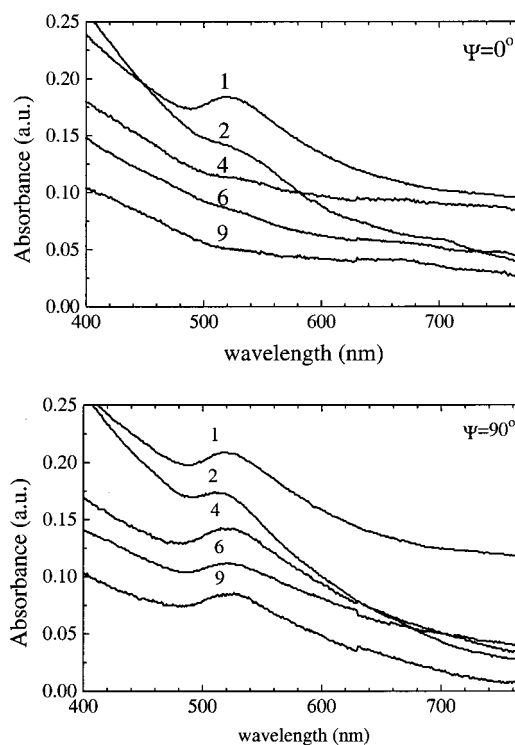*J. Phys. Chem. B, Vol. 103, No. 28, 1999* **5765**

Figure 6. The polarization spectra of the $L/d = 4.4$ rods dispersed in PVA for various elongation numbers indicated on the spectral curves. The curves are arbitrarily shifted along the *y*-axis for the sake of clarity. The polarization angle, Ψ, is given in the figures. Note that the spectra are split in two wavelength regimes. The wavelength regime 400−800 nm is shown on the left-hand side and the wavelength regime 750−1250 nm on the right-hand side.

9. The gold concentration of this particular film is estimated to be 170 μg·cm^{-2}. These CSLM micrographs clearly demonstrate that by stretching the film the colloidal gold rods gradually align parallel to the stretch direction. In the first image (Figure 8a) the random distribution of single rods is observed in the unstretched film. The second image (Figure 8b) shows a small increase in orientational ordering in the stretch direction. The elongation is between 1 and 3 at this place in the film. The third image (Figure 8c) is taken at the position where the elongation was 3. Some disorder in orientation can still be noticed, but a strong preferential orientation in the stretch direction is present. The last picture (Figure 8d) shows the film which was stretched 9× and a complete alignment of the gold rods is clear.

The CSLM micrographs also illustrate that the colloidal gold rods are homogeneously dispersed in the PVA film and that hardly any clusters are present. The CSLM images thus support the conclusion that the aqueous and PVA dispersion of rod-shaped gold particles are colloidally stable. In the case of a considerable amount of aggregates in the aqueous solution, the PVA film should consist of these aggregates as well.

Conclusions

The absorbance spectra of the random systems comply with the theoretical predictions, indicating that the gold rods are well-dispersed in PVA, which is supported by CSLM analysis. The optical behavior of the random systems changes markedly by stretching the PVA films. The anisotropic gold particles are completely aligned as a result of stretching. Consequently, the absorbance becomes sensitive to the polarization direction.

Figure 7. The polarization spectra of the $L/d = 17.2$ rods dispersed in PVA for various elongation numbers indicated on the spectral curves. The curves are arbitrarily shifted along the *y*-axis for the sake of clarity. The polarization angle, Ψ is given in the figures. Note that the longitudinal resonance falls outside the scope of the wavelength regime.
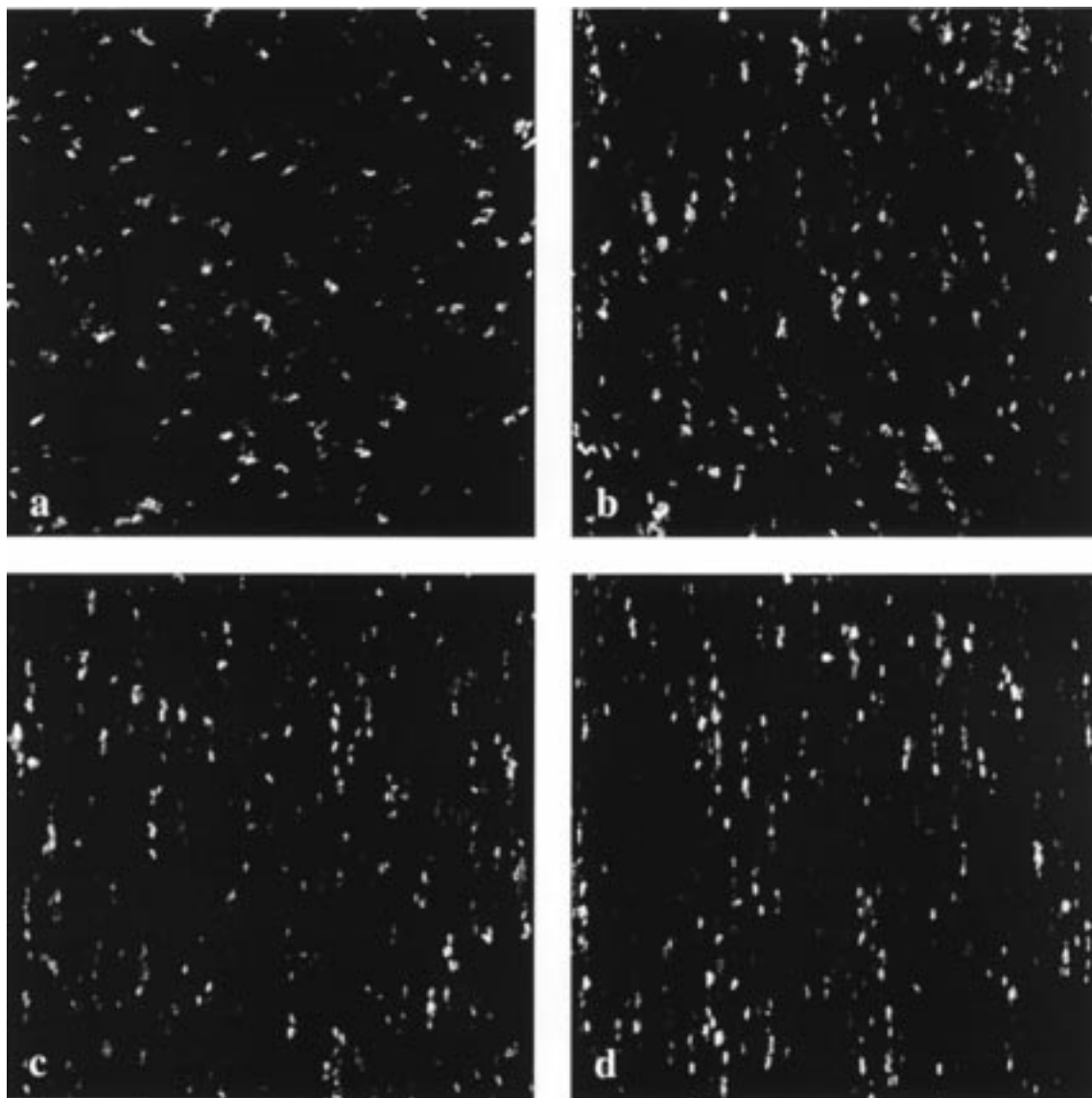
Figure 8. Sequence of CSLM micrographs of the PVA film containing gold rods with $L/d = 49$ demonstrating the gradual alignment with increasing elongation: (a) the unstretched film and for elongation numbers (b) 1–3, (c) 3, and (d) 9. Image size 50×50 μm.

When the electric field of the incident light is polarized parallel to the main axis of the particle, the absorbance spectrum shows only the longitudinal resonance. Conversely, when the electric field of the incident light is polarized perpendicular to the main axis the absorbance is caused by the transverse resonance. Complete alignment of the anisotropic particles is obtained after the PVA film is stretched 4–6 times its original length. No significant effect of the aspect ratio is observed on the film elongation for complete alignment. CSLM amplifies the conclusions drawn from the polarization spectra and visualizes the orientation of the gold rods in the continuous phase as function of the elongation.

Appendix I

Gans[13−15] derived an expression to describe the interaction of light with an elongated ellipsoids (or rods) by introducing a geometrical factor P_j corresponding to each of the axes A, B, and C of the particle. Gans' formula for randomly oriented, elongated ellipsoids in the dipole approximation is

$$\frac{\gamma}{N_p V} = \frac{2\pi\epsilon_\alpha^{3/2}}{3\lambda} \sum_{j=A}^{C} \frac{\left(\frac{1}{P_j^2}\right)\epsilon_2}{\left[\epsilon_1 + \left(\frac{1-P_j}{P_j}\right)\epsilon_\alpha\right]^2 + \epsilon_2^2} \quad (a1)$$

Here, ϵ_1 and ϵ_2 represent the real and the imaginary part of the complex dielectric function, respectively, λ the wavelength of light in vacuum, ϵ_α the dielectric constant of the surrounding medium, N_p the number concentration of particles, V the single particle volume, and γ is the extinction coefficient.

For elongated ellipsoids (or rods) the B and C axis correspond to the particle diameter, while the A axis represents the particle length L. The geometrical factors P_j for elongated ellipsoids

Optical Properties of Aligned Au Particles

J. Phys. Chem. B, Vol. 103, No. 28, 1999 **5767**
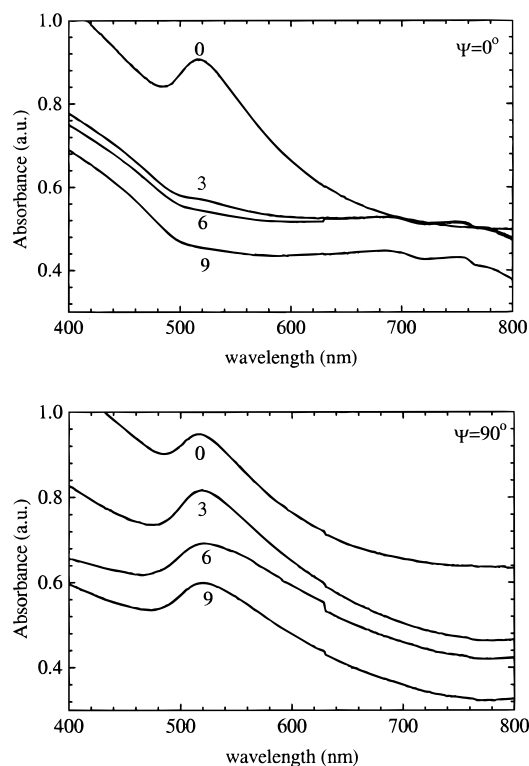
Figure 9. The polarization spectra of the $L/d = 49$ rods dispersed in PVA. The curves are arbitrarily shifted along the y-axis for the sake of clarity. The polarization angle, Ψ, is given in the figures. Note that the longitudinal resonance falls outside the scope of the wavelength regime.

along the A and B/C axis are defined as[14]

$$P_A = \frac{1 - e^2}{e^2}\left[\frac{1}{2e}\ln\left(\frac{1 + e}{1 - e}\right) - 1\right] \qquad (a2)$$

$$P_B = P_C = \frac{1 - P_A}{2} \qquad (a3)$$

with

$$e = \left(\frac{L^2 - d^2}{L^2}\right)^{1/2} \qquad (a4)$$

The wavelength at which the plasmon resonates is determined by the denominator in eq a1 and occurs if

$$\epsilon_1 + \left(\frac{1 - P_j}{P_j}\right)\epsilon_\alpha = 0 \qquad (a5)$$

Here, $(1 - P_j)/P_j$ is called the screening parameter, κ_j, which strongly depends on the aspect ratio of the particle. Two values of the screening parameter exist for rods. With increasing aspect ratio the screening parameter (κ_A) of the longitudinal oscillation is shifted toward infinity, while in the case of the transverse oscillation the screening parameter ($\kappa_B = \kappa_C$) reaches one. The two values of κ_j lead to two absorbance peaks that positions of which depend strongly on the aspect ratio of the particles.

References and Notes

(1) Creighton, J. A.; Eadon, D. G. *J. Chem. Soc., Faraday Trans.* **1991**, *87*, 3881.

(2) Dauchot, J.; Watillon, A. *J. Colloid Interface Sci.* **1967**, *23*, 62.

(3) Mulvaney, P. *Langmuir* **1996**, *12*, 788.

(4) van der Zande, B. M. I.; Böhmer, M. R.; Fokkink, L. G. J.; Schönenberger, C. *J. Phys. Chem. B* **1997**, *101*, 852.

(5) van der Zande, B. M. I.; Böhmer, M. R. Submitted to Langmuir.

(6) Tanori, J.; Pileni, M. P. *Langmuir* **1997**, *13*, 639.

(7) Esumi, K.; Matsuhisa K.; Torigoe, K. *Langmuir* **1995**, *11*, 3285.

(8) Yu, Y.; Chang, S.; Lee, C.; Wang, C. R. *J. Phys. Chem. B.* **1997**, *101*, 6661.

(9) Lickes, J.-P.; Dumont, F.; Buess-Herman, C. *Colloids Surf. A: Physicochem. Eng. Aspects* **1996**, *118*, 167.

(10) Lisiecke, I.; Billoudet, F.; Pileni, M. P. *J. Phys. Chem.* **1996**, *100*, 4160.

(11) Lebedeva, V. N.; Distler, G. I. *Opt. Spectrosc.* **1967**, *23*, 527.

(12) Skillman, D. C.; Berry, C. R. *J. Phys. Chem.* **1968**, *48*, 3297.

(13) Gans, R. *Ann. Physik* **1912**, *37*, 881; **1915**, *47*, 270.

(14) Papavassiliou, G. C. *Prog. Solid. State Chem.* **1979**, *12*, 185.

(15) Bohren, C. F.; Huffman, D. R. *Absorption and scattering of light by small particles*; Wiley: New York, 1983.

(16) Fornasiero, D.; Grieser, F. *Chem. Phys. Lett.* **1987**, *139*, 103.

(17) Thulstrup, E. W.; Michl, J.; Eggers, J. H. *J. Phys. Chem.* **1970**, *74*, 22.

(18) van Zandvoort, M. A. M. J. Pigment-polymer matrixes as model systems for energy transfer processes between photosynthetic pigments. Thesis, Utrecht University, The Netherlands, 1994.

(19) van der Zande, B. M. I.; Koper, G. J. M.; Lekkerkerker, H. N. W. *J. Phys. Chem. B* **1999**, *103*, 5754 (preceding paper in this issue).

(20) Al-Rawashdeh, N. A. F.; Sandrock, L.; Seugling, C. J.; Foss, C. A., Jr. *J. Phys. Chem. B* **1998**, *102*, 361.

(21) Wilson, T. *Confocal microscopy*; Academic Press: London, 1990.

(22) van Blaaderen, A. *Adv. Materials* **1993**, *5*, 52.

(23) van der Zande, B. M. I.; Böhmer, M. R.; Fokkink, L. G. J.; Schönenberger, C. Submitted to Langmuir.

(24) van der Zande, B. M. I.; Dhont, J. K. G.; Böhmer, M. R.; Philipse, A. P. Submitted to Langmuir.

(25) Frens, G. *Nature (London), Phys. Sci.* **1973**, *241*, 20.

(26) Lide, D. R. *Handbook of chemistry and physics*, 73th ed.; CRC Press, Inc.: Boca Raton, FL, 1992−1993.

(27) Nomura, S.; Kawai, H. *J. Pol. Sci., Part A-2* **1966**, *4*, 797.

(28) Foss, C. A.; Hornyak, G. L.; Stockert, J. A.; Martin, C. R. *J. Phys. Chem.* **1994**, *98*, 2963.

(29) Maxwell−Garnett, J. C. *Philos. Trans. R. Soc.* **1904**, *302*, 385.

(30) Doremus, R. H. *J. Colloid Interface Sci.* **1968**, *27*, 412.

(31) *Optical properties of metals*; Weaver, J. H., Krafka, C., Lynch, D. W., Eds.; Physics Data Series, No. 18-2; Fachinformationzentrum: Karlsruhe, 1981; Vol. 2.

(32) Guraljani, M. L.; Padhye, M. R. *Indian J. Technol.* **1971**, *9*, 211.

(33) Morgan, H. M. *Textile Res. J.* **1962**, *32*, 866.